Self-Assembly and Metalation of pH-Sensitive Double Hydrophilic Block Copolymers with Interacting Polymer Components

Nataliya Permyakova, Tatyana Zheltonozhskaya, Olga Revko, Lyudmila Grischenko*

Summary: Double hydrophilic diblock copolymers (DBCs) contained chemically complementary methoxypoly(ethylene oxide) and poly(acrylic acid) (MOPEO-*b*-PAAc) with the constant length of MOPEO block ($M_{vMOPEO} = 5$ kDa) and variable length of polyacid block ($M_{nPAAc} = 9.9 \div 23.1$ kDa) were synthesized by a free radical block copolymerization of PAAc with methoxypoly(ethylene glycol) (MOPEG). These copolymers were pH-sensitive in aqueous medium, namely, at low pH the polyacid blocks were protonated and formed the intramolecular polycomplexes with MOPEO blocks that resulted in an intense micellization initiated by hydrophobic interactions between non-polar bound segments of the blocks. Hydrophobic ''core'' of the micelles comprised H-bonded segments of MOPEO and PAAc blocks while hydrophilic ''corona'' included the surplus units of longer blocks. The capability of DBCs as templates for the silver nanocluster/nanoparticle is considered. The kinetics of the Ag-nanoparticle growth in the copolymer matrices and optical properties of nanoclusters and nanoparticles were determined and discussed.

Keywords: diblock copolymers; micelles; nanoparticles; self-assembly; silver

Introduction

It is well known that amphiphilic block copolymers form different micellar structures in dilute solutions of the solvents, which are selective for one of the blocks.[1] Polymeric micelles contain a dense ''core'' formed by segregation of insoluble blocks and a swelled ''corona'' with soluble blocks that ensures stabilization to whole micellar structure. Many double-hydrophilic block copolymers are known to be a stimuli responsive copolymers, respond to changes in the solution pH, temperature, salt concentration and so on.[2–6] pH-sensitive block copolymers would contain ionic groups, which ionization is dependent on pH. There are several studies devoted to the micellization process of pH-sensitive diblock copolymers and concerned to the influence of polymeric structure, the solution pH and ionic strength on micellar characteristics.[2,5] The pH-dependent micellization of diblock copolymers containing hydrophilic chemically complementary blocks, which are capable of ''self-complexation'',[3,6] is of particular interest. We reported recently that the double hydrophilic block copolymers with the system of cooperative hydrogen bonds between chemically complementary polymeric blocks formed stable micelles in aqueous medium.[7,8] This special type of micelles contains hydrophobic ''core'' with H-bonded segments of interacting blocks and hydrophilic ''corona'' with free (unbound) segments of longer blocks. The given micellar structures have attracted a considerable attention due to

Kiev National Taras Shevchenko University, Faculty of Chemistry, Department of Macromolecular Chemistry, 60 Vladimirskaya St., 01033 Kiev, Ukraine
E-mail: permyakova@ukr.net

their possible applications as different templates, drug delivery systems, nanoreactors, components of membranes etc.[2,5]

In this paper, we represented: i) peculiarities of a synthesis of diblock copolymers (DBCs) contained chemically complementary methoxypoly(ethylene oxide) of the constant chain length and poly- (acrylic acid) (MOPEO-*b*-PAAc) with a different length of polyacid block, ii) self-assembly of the copolymers in aqueous solutions, and iii) the process of silver nanoparticle formation in DBC matrices as a function of the solution pH. Stabilizing action of DBCs in respect of the growing silver nanoclusters/nanoparticles is considered.

Peculiarities of Syntheses

The MOPEO-*b*-PAAc block copolymers were synthesized by a free radical block copolymerization of acrylic acid (AAc) (''Fluka'', USA), distilled under vacuum, with MOPEG ($M_v = 5$ kDa) from the same firm. Hydroxyl groups of MOPEG were activated by cerium ammonium nitrate.[9] The block copolymerization was performed at the constant molar ratio $[Ce^{IV}]/[MOPEG] = 1$ and a variable monomer concentration in the reaction mixture (from 0.5 to 2.0 mol_{AAc}/base-mol_{MOPEG}). The process was accompanied by a phase separation. A pure PAAc was obtained by a free radical homopolymerization of AAc in the same experimental conditions at the presence of ethanol instead MOPEG ($[AAc]/[EtOH] = 0.5 \div 2$). The (co)polymerization rate and the monomer conversion in both the processes were controlled by potentiometric titration. A certain volume of the reaction mixture (~2 ml) was taken through a definite time of the process. Potentiometric titration of the non-reacted AAc was performed by 0.2 N NaOH in an inert atmosphere at $T = 25 \pm 0.1\ ^\circ C$ using a 1–160M pH-meter (Belarus) calibrated with standard buffers.

The essential increase in the (co)polymerization rate and the monomer conversion during the block copolymerization process as compared to AAc homopolymerization, that was observed at relatively low monomer concentrations (Figure 1a, b), pointed out the positive dynamic template effect.[10] At $[AAc]/[MOPEG] = 2.0$, the kinetic curves for both the processes were drawn together, thus implying disappearance of the positive dynamic template effect (Figure 1c). More clearly this situation is highlighted by the data of Table 1, which were calculated from Figure 1.

It is seen from Table 1 that the rate of both the processes significantly increased with the growth of the monomer concentration up to 1.46 $mol \cdot dm^{-3}$. In our previous study[8], we observed analogous positive template effect at the block copolymerization of PAAc with MOPEG samples of less molecular weights ($M_{vMOPEG} = 1.1$ and 2 kDa) at similar low monomer concentrations.

Thus, it was revealed that the block copolymerization process had the template

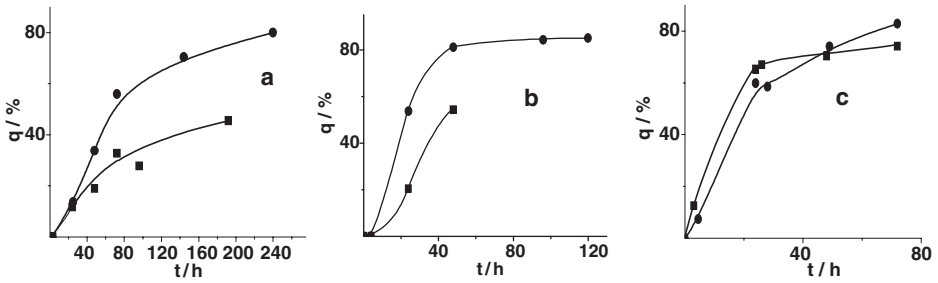

Figure 1.
The time–conversion curves for the ratios: (**a**) 0.5, (**b**) 1.0, and (**c**) 2.0 mol_{AAc}/base-mol_{MOPEG}; ■ = homopolymerization, ● = block copolymerization; $T = 20\ ^\circ C$.

Table 1.
Kinetic parameters of homopolymerization and block copolymerization.

Sample	C_{AAc} mol · dm^{-3}	[AAc]/[MOPEG][a] mol/base-mol	$V_p^{20} \cdot 10^{6}$[b] mol/(dm^3 · s)	$V_p^{40} \cdot 10^{6}$ mol/(dm^3 · s)	q[c] %
DBC1	0.37	0.5	0.86	0.93	72
PAAc1			0.47	0.07	34
DBC2	0.73	1	5.6	6.5	81
PAAc2			2.4	3.1	54
DBC3	1.46	2	10.72	10.72	73
PAAc3			10.99	10.91	71

[a] [AAc]/[EtOH] for the PAAc homopolymerization. [b] The rate of (co)polymerization at the monomer conversion equaled to 20% and 40%. [c] The monomer conversion in 48 hours after the (co)polymerization beginning.

character only at a relatively low monomer concentration in the reaction mixture ($C_{AAc} < 1.46$ mol · dm^{-3}). When the monomer concentration in the reaction mixture turned out higher than 1.46 mol · dm^{-3}, the rate of copolymerization process was increased so strongly that the growing PAAc chains had not enough time to interact with the template blocks of MOPEO. According to the studies,[10] the template effect is caused by the formation of the H-bond system between the propagating (''daughter's'') PAAc chains and MOPEO blocks.

The sediments of DBCs in H-form were rewashed after syntheses by the deionized water and transformed to Na-form by dissolution in water with sodium hydroxide. The obtained DBCs in Na-form were reprecipitated by the addition of hydrochloric acid up to pH = 2; then they were dissolved again in the sodium hydroxide solution and freeze dried. A single DBC sample in H-form ($DBC_{PAAc}2$) synthesized at C_{AAc} = 0.73 mol · dm^{-3} was transformed to Na-form and precipitated by hydrochloric acid also. But unlike to other two copolymer samples ($DBC_{PANa}1,3$), this sample was dissolved in ethanol and was dried using the rotor evaporator.

Chemical Composition and Bulk Structure

Molecular parameters of DBCs and their chemical compositions were determined by ^{1}H NMR spectroscopy as in the study.[11] ^{1}H NMR spectra of $DBC_{PAAc/PANa}$ were recorded with a 400 MHz Mercury-400 spectrometer from ''Varian'' (USA) at T = 20 °C using DBC_{PAAc} solutions in DMSO-d_6 and DBC_{PANa} solutions in D_2O with C = 1 kg · m^{-3} (Figure 2).

The 1H NMR spectrum of DBCPANa3 showed two resonance signals of MOPEO block with the chemical shifts δ = 3.66 and 3.37 ppm, which could be attributed to the protons of methylene (b) and methoxy groups (a) and two groups of signals for PANa block with the chemical shifts δ = 1.44 and 2.05 ppm, which ones corresponded to the protons of methylene (c) and methyne (d) groups.[17] The number average molecular weights of MOPEG (M_{nMOPEG}) and PAAc/PANa blocks (M_{nPAAc} or M_{nPANa}) in DBCs were calculated according to the ratio of the integral intensities of corresponding proton signals as in the studies.[8,11] The molecular weight of PAAc was determined by viscometry (Table 2). Note that the copolymer compositions were in a good agreement with the targeted values.

Structural peculiarities of initial MOPEG and DBCs in H- and Na-forms were studied by differential scanning calorimetry (DSC). DSC thermograms of DBCs are represented in Figure 3 but corresponding parameters of thermal transitions are shown in Table 3.

DSC curves for DBCPAAc2 (the 1-st and 2-nd scans) showed only single capacity jumps at Tg = −3.1 °C and −5.5 °C (Table 3), which could be assigned to the glass transitions in the amorphous regions

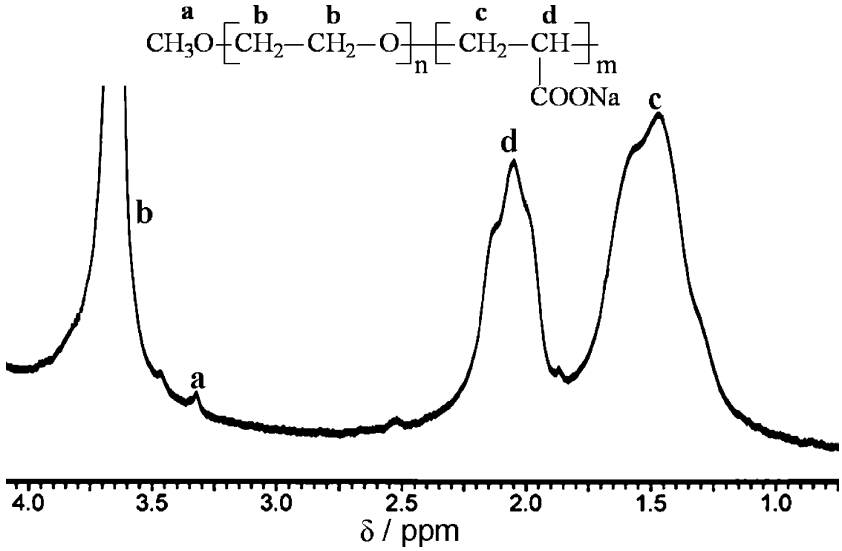

Figure 2.
^{1}H NMR spectrum for $DBC_{PANa}3$ in D_2O.

Table 2.
Characterization of the diblock copolymers and a pure polyacid.

Polymer	M_{vMOPEG} kDa	M_{nMOPEG} [a)] kDa	$M_{nPAAc/PANa}$ kDa	M_{nDBC} [b)] kDa	n[c)]
$DBC_{PANa}1$	5.00	5.29	9.98	15.27	106/120
$DBC_{PAAc}2$	5.00	5.28	6.52	11.80	91/120
$DBC_{PANa}3$	5.00	5.29	23.05	28.34	245/120
PAAc3	–	–	22.00[d)]	–	–

[a)] $M_{nMOPEG} = (3 \cdot M_{oMOPEG} \cdot A_b)/4 \cdot A_a$, where M_{oMOPEO} is the molecular weight of MOPEO (or MOPEG) units, A_b and A_a are the integral intensities of the proton signals of methylene and methoxy groups of MEPEG. [b)] $M_{nDBC} = M_{nMOPEO} + M_{nPANa(PAAc)}$. [c)] The ratio between repeat units of the blocks (base-$mol_{PANa(PAAc)}$/base-mol_{MOPEO}). [d)] The value of M_v was found by viscometry.

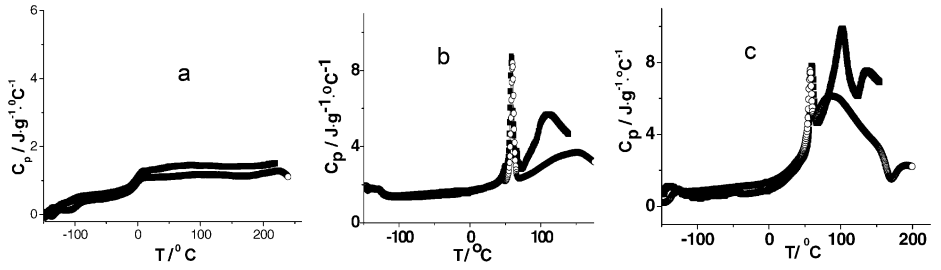

Figure 3.
DSC thermograms for: (**a**) $DBC_{PAAc}2$, (**b**) $DBC_{PANa}1$ and (**c**) $DBC_{PANa}3$; ■ = the 1-st scan, ○ = the 2-nd scan.

of the copolymers. One glass transition is typical also for individual PAAc, but its Tg value lies in higher temperature region (109–125 °C).[12,13] The intense melting peak, which was characteristic for initial MOPEG (Table 3), was absent in these DSC thermograms (Figure 3a). This effect together with a sharp decrease in Tg value

Table 3.
Parameters of thermal transitions in the structure of diblock copolymers.

Polymer	Scan	T_g [a] °C	ΔT_g [b] °C	ΔC_p [c] J/g °C	T_m [d] °C	ΔT_m [e] °C	ΔH_m [f] J/g	X_c [g] %
MOPEG	1	–	–	–	61.5	48.9	196.8	100.0
	2	–	–	–	59.5	56.7	175.9	89.4
$DBC_{PAAc}2$	1	−3.1	25	0.58	–	–	–	–
	2	−5.5	24	0.55	–	–	–	–
$DBC_{PANa}1$	1	–	–	–	58.9	36.0	41.0	60.1
	2	–	–	–	60.1	48.0	31.2	45.8
$DBC_{PANa}3$	1	–	–	–	59.8	20.0	20.3	55.3
	2	177.5	13	0.81	57.4	16.6	17.1	46.5

[a]The glass transition temperature.[b]The interval of glass transition.[c]The specific capacity jump.[d]The melting temperature.[e]The interval of melting transition.[f]The melting enthalpy.[g]The crystallinity degree for MOPEO block in DBC: $X_c = \Delta H_m/\Delta H^o_m$, where $\Delta H^o_m = 196.8\ J \cdot g^{-1}$ is the melting enthalpy for 100% crystalline PEO.[14]

for DBCPAAc2 as compared to PAAc could be attributed to the whole compatibility of both the blocks in DBCPAAc2 structure that is conditioned by the formation of H-bond system between MOPEO and PAAc blocks.[7]

One is known that the presence of sodium acrylate units in PAAc strongly increase the rigidity of polyacid chains that is accompanied by essential enhance in T_g values. Similar behavior is not characteristic for conventional copolymers based on non-ionic species.[15] Indeed, ionic interactions are among the strongest known types of forces that may exist between molecules. The presence of ionic groups in the copolymer promotes the formation of ion-rich aggregates in the non-polar polymer matrix. These ion-rich aggregates lead to a variety of ionic interactions that change the polymer properties. In turn, these interactions depend on the degree of neutralization.[15] The glass transition temperature for homopolymer PANa lies in the region of 230–250 °C.[16] The adsorbed water is known strongly reduces T_g value for PANa.[16]

Unlike to $DBC_{PAAc}2$, DSC thermograms for $DBC_{PANa}1,3$ (the 1-st scans) revealed some endothermic peaks. The first peak corresponded to the melting process in crystalline domains formed by MOPEO blocks but the second one reflected the evaporation of the immobilized (~100 °C) and adsorbed (~137 °C) water. The parameters ΔH_m and X_c for MOPEO blocks in DBCs turned out to be less than those for individual MOPEG that could be explained by the reduction in MOPEO crystallinity in the copolymer structure. DSC thermogram for DBCPANa3 (the 2-nd scan) demonstrated besides melting peak of MOPEO crystalline domains also one glass transition with Tg = 177.5 °C (Table 3). Such effects pointed out a thermodynamic immiscibility of MOPEO and PANa blocks and a microphase separation in DBCPANa structure.

Micellization as a Function of the Solution pH

The template character of the block copolymerization process pointed out the existence of the intramolecular polycomplexes (IntraPCs) in DBC_{PAAc} macromolecules in H-form due to formation of H-bonds between growing PAAc chains and MOPEO blocks[7]. Micellization of these DBCs in aqueous solutions develops because of hydrophobic segregation of non-polar bound parts of the copolymer blocks. At the same time, the IntraPC formation and micellization is impossible in the case of fully deprotonated DBC_{PANa} copolymers. We studied DBC micellization as a function of the solution pH using Vis spectroscopy, photography and static light scattering (SLS). Corresponding pH values and the dissociation degrees (α) of carboxylic groups were obtained from the data

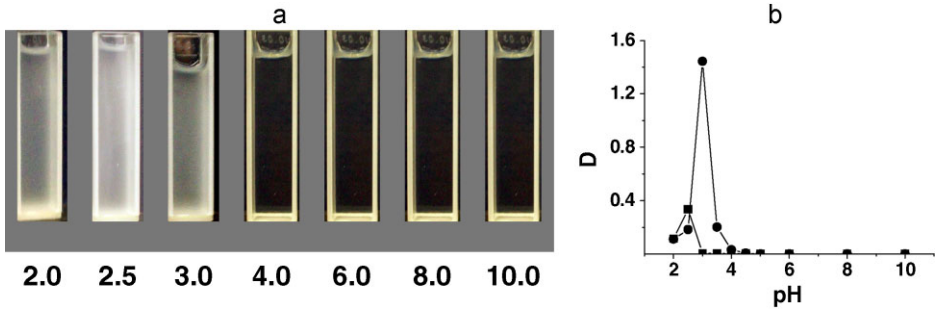

Figure 4.
(**a**) Photos and (**b**) the optical density (tubidity) of $DBC_{PANa/PAAc}3$ solutions at different pH; ■ $C = 1\ kg \cdot m^{-3}$ (**a**, **b**), • $C = 2\ kg \cdot m^{-3}$ (**b**), $\lambda = 500$ nm.

of potentiometric titration. Optical density (tubidity) of $DBC_{PANa/PAAc}$ solutions at different pH was carried out on a UV/Vis spectrometer Perkin Elmer Lambda 20 (Sweden) at $\lambda = 500$ nm. Some results are shown in Figure 4.

The appearance of turbidity in DBCPANa3 dilute solutions at $pH \leq 4$ indicated a self-assembly of the copolymer macromolecules due to: i) IntraPC formation and ii) hydrophobic segregation.[3,7] The following decrease in the solution pH resulted in a sharp growth in the solution turbidity (Figure 4) that was conditioned by the increase in the quantity of H-bonds between the blocks and further development of the micellization process. At the destruction of H-bond system in IntraPCs at $pH > 4$ the micelle ruining takes place. A scheme of the micellization process is represented below but specific construction of the micelles in the case of asymmetric block copolymers with chemically complementary components was discussed above.

In order to compare the micellization process for two asymmetric DBCs (the samples 1 and 3) with different relative length of the blocks and to determine by SLS method the critical micellization concentrations (*CMC*) at $pH = 2.5$, we used a modernized instrument FPS-3 (Russia), which was equipped by a light diode WP7113VGC/A ($\lambda = 520$ nm) from ''Kingbright'', the controller ADC-CPU™ from ''Insoftus'' (Ukraine) and the computer program ''WINRECORDER''. The *CMC* determination is shown in Figure 5a. It should be noted an essential intensification of the micellization process at the reduction in the asymmetry of DBC blocks. Indeed, the micellization developed more intensively, when the unit ratio in DBC_{PAAc} was 100/113 (unlike to 234/113).

Such conclusion was confirmed by the values of *CMC* and the Gibb's free micellization energy (calculated by the relation: $\Delta G^0 \approx RT\ \ln CMC$ [17]), which are represented in Table 4.

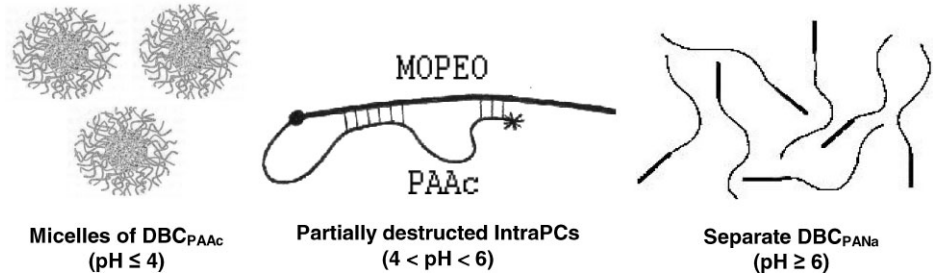

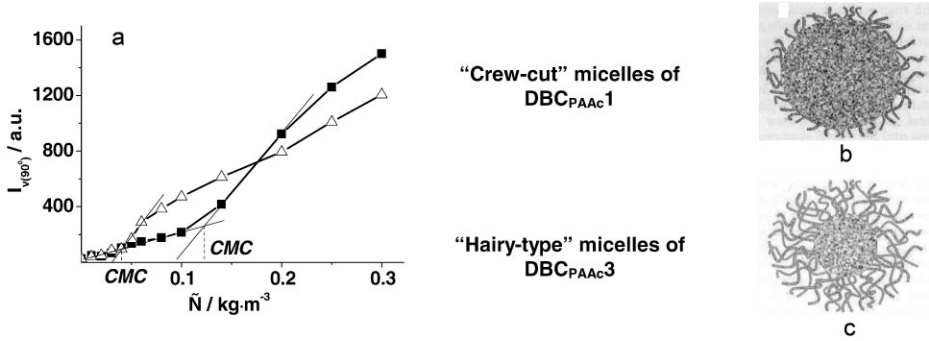

Figure 5.
(**a**) The scattered intensity of the vertically polarized light at the $\theta = 90^\circ$ scattering angle *vs* DBC_{PAAc} concentration at pH = 2.5; Δ = $DBC_{PAAc}1$, ■ = $DBC_{PAAc}3$. Schemes of micelle building for (**b**) $DBC_{PAAc}1$ and (**c**) $DBC_{PAAc}3$.

Table 4.
Thermodynamic parameters of the copolymer micellization at pH = 2.5

Copolymer[a)]	n	CMC mol/dm^3	$-\Delta G^\circ$ kJ/mol
$DBC_{PAAc}1$	106/120	2.85	31.32
$DBC_{PAAc}3$	245/120	4.56	30.16

[a)]Initial designations of the copolymers $DBC_{PANa}1,3$ were changed by $DBC_{PAAc}1,3$ because of practically full protonation of polyacid blocks at pH = 2.5.

One could be assumed that $DBC_{PAAc}1$ macromolecules formed spherical ''crew-cut'' micelles[1,17] contained a large hydrophobic ''core'' with H-bonded segments of the blocks and a short ''corona'' with free nonionic segments of MOPEO blocks (Figure 2b).

The alternative micellar structure could be attributed to $DBC_{PAAc}3$, which contained a significant excess of unbound units of PAAc blocks (Figure 2c). In this case, the formation of ''hairy-type'' micelles[1] with relatively small hydrophobic ''core'' and a large ''corona'' would be expected.

Interaction with Silver Ions

Studying the silver ion interaction with the block copolymers was an important stage to understand the processes, which take place at the formation of Ag-nanoparticles in DBC solutions. For this purpose Ag^+-containing DBC_{PANa} were prepared by mixing aqueous solutions of the copolymers with silver nitrate (at different molar ratios between Ag^+ ions and carboxylate groups) followed by their keeping at a room temperature during 1 h. The interaction of Ag^+ with DBC_{PANa} we observed by an appearance of the solution turbidity, which essentially strengthened with growth of Ag^+ concentration. The nature of this interaction was studied by FTIR spectroscopy. FTIR spectra of thin (3–7 μm) films of one of the copolymers and its mixture with silver salt at pH = 9.6, which ones were prepared on fluorite glasses and dried on air and under vacuum during one week, were recorded by a ''Nexus-470 Nicolet'' spectrometer (USA) with a resolution 4 cm^{-1} at 20 °C (Figure 6). There are two character-

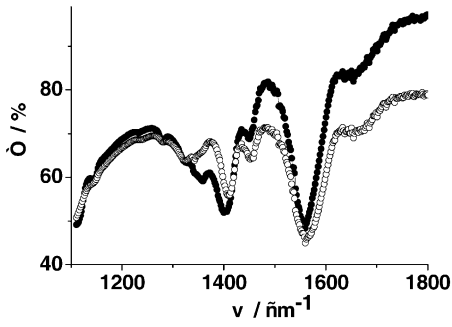

Figure 6.
FTIR spectra of $DBC_{PANa}3$ and its blend with Ag salt at the molar ratio $[Ag^+]/[COO^-] = 0.4$; ○ = $DBC_{PANa}3$, • = $Ag^+/DBC_{PANa}3$ blend; T = 20 °C.

istic intense vibration bands in $DBC_{PANa}3$ spectrum at 1410 and 1560 cm^{-1}, which corresponded to symmetric (ν_{sCOO}-) and asymmetric (ν_{asCOO}-) vibrations of carboxylate ions, consequently.[18,19] The distance ($\Delta\nu$) between their positions was not changed in the spectrum of Ag^+/DBC blend at the molar ratio $[Ag^+]/[COO^-] = 0.1$. However, this value increased in 10 cm^{-1} at the growth of the $[Ag^+]/[COO^-]$ ratio up to 0.4.

This effect is known to indicate the connection of metal ions with carboxylate groups.[18] Thus, one can conclude that Ag+ ions stronger interact with COO- groups than Na+ ones.

Formation of Silver Nanoparticles in DBC Solutions

One of the most common methods to prepare silver nanoparticles is chemical reduction of silver ions by a strong agent such as sodium borohydride.[20–22] Syntheses of silver nanoparticles in DBC solutions were carried out by the addition of $NaBH_4$ (from China) to Ag^+/DBC blends ($C_{DBC} = 1\ kg \cdot m^{-3}$) at a molar ratio of $[Ag^+]/[COO^-] = 0.1$. The excess of the reducing agent is necessary to favor the formation of monodispersed metal nanoparticles through a fast nucleation process.[22] This process could be described by the (1) stochiometric equation:[21]

$$8Ag^+ + BH_4^- + 8OH^- = 8Ag + H_2BO_3^- + 5H_2O \quad (1)$$

In our experiments the excess of $NaBH_4$ with respect to Ag^+ ions was 8–80 times. The Ag nanoparticles were identified using UV-Vis spectroscopy. Corresponding spectra of the reaction mixtures were recorded by a ''Cary 50 Scan UV-Visible Spectrophotometer'' from ''Varian'' (USA) in the 200–1000 nm region.

The chemical reduction of silver ions by $NaBH_4$ (at $[NaBH_4]/[Ag^+] = 80$) in $DBC_{PANa/PAAc}$ solutions happened in a moment. During 5 minutes, a color of the reaction mixtures gradually changed. The effect depended on the solution pH. So, Ag^+/DBC_{PANa} mixture with pH = 9.6 showed a yellow color, while analogous mixture with pH = 2.5 demonstrated a blue one. During reaction time (2 h) the colors of both the mixtures darkened. The yellow color is known to correspond to formation of Ag-nanoparticles but the blue one means the appearance of silver nanoclusters and their complexation with polyelectrolyte chains.[18] Nano-scaled metal particles exhibit an intense band of the surface plasmon resonance, which is conditioned by the movement of conducting electrons at the particle surface.[22] In our case the absorption band with λ_{max} near 400 nm characterizes the surface plasmon resonance of Ag-nanoparticles.[20–22] According to the studies,[22,23] the band position, the absorption maximum and the band shape depend on particle size, form, polydispersity and surrounding medium. Typical plasmon resonance bands, which were recorded during the process of Ag-nanoparticle synthesis in $DBC_{PANa}3$ solutions, are shown in Figure 7.

We observed a steady increase in the intensity of the absorption band with $\lambda_{max} = 381$ nm at earlier reaction stages and further decrease in the band intensity and its red shift in 27–29 nm (up to $\lambda_{max} = 408$–410 nm) at longer time. Then

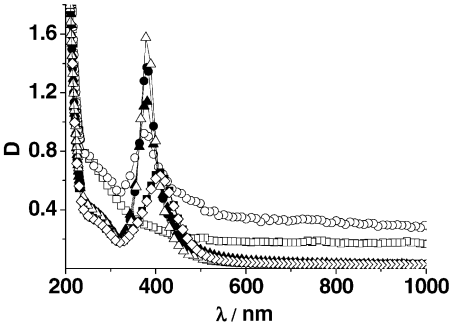

Figure 7.
Absorption spectra of Ag-nanoparticles obtained in $DBC_{PANa}3$ solution in different time after reduction beginning; □ = 5, ○ = 15, ▲ = 35, • = 120, Δ = 270, ■ = 5760, ◇ = 14400 min; $C_{DBC} = 1\ kg \cdot m^{-3}$, $C_{AgNO_3} = 1.4 \cdot 10^{-2}\ kg \cdot m^{-3}$, $[NaBH_4]/[Ag^+] = 80$.

the position of the band did not change for a long time. According to the Mie's theory,[24] the observed plasmon resonance band would correspond to the particles, whose size is less than ~30 nm. When the reaction time exceeded 270 min, the maximum intensity of the plasmon band was reached. Increasing in the band intensity at practically constant λ_{max} values could be attributed to the growth of nanoparticle quantity. Kinetic peculiarities of Ag-nanoparticle growth in DBC_{PANa} solutions are represented in Figure 8 as the time evolution of the absorption maximum (D_{max}) at λ_{max} (Figure 8a, b), the position (λ_{max}) of the plasmon resonance band (Figure 8c, d), and the integral intensity of this band (Sq) (Figure 8e), which is proportional to the yield of Ag-nanoparticles.

Note, that in UV region of the spectra a weak absorption band with λ_{max} = 270–290 nm, which corresponded to the nanoclusters Ag_4^{2+},[21] were also displayed (Figure 7). Based on these data, one can assume that the particle formation is

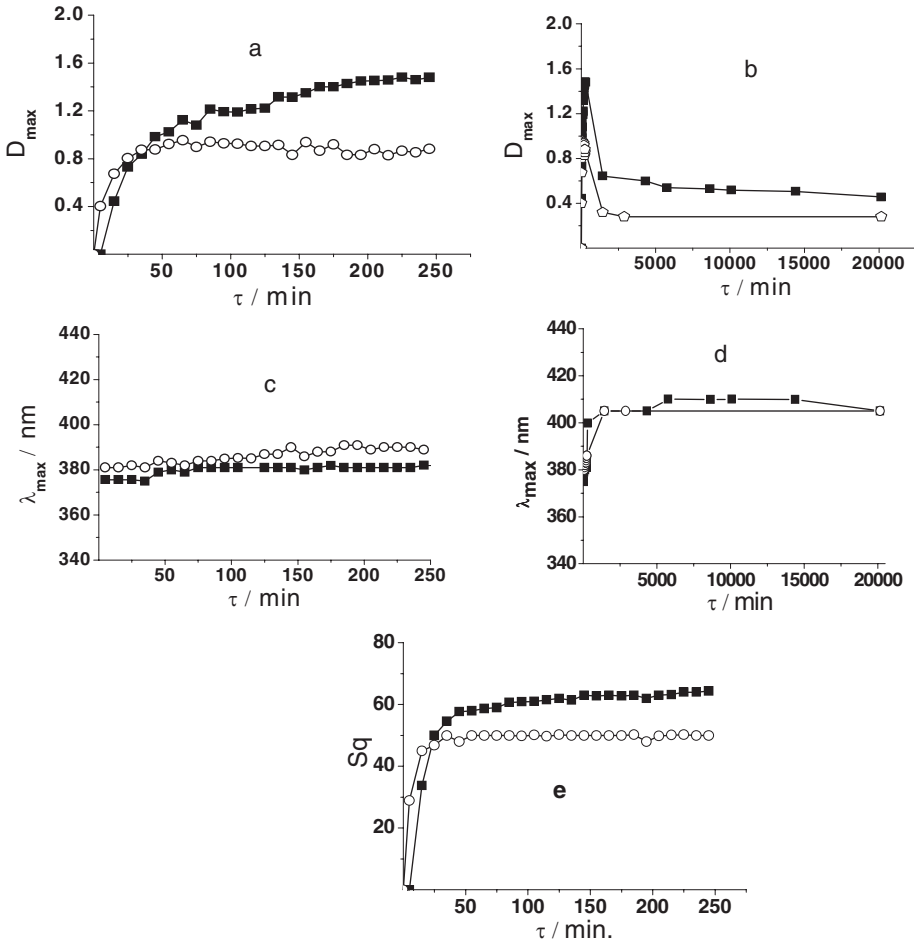

Figure 8.
Time dependences of (a, b) the absorption maximum (Dmax), (c, d) the position (λmax) and (e) the integral intensity of the plasmon resonance band for Ag-nanoparticles formed in DBCPANa solutions; ○ = DBCPANa1, ■ = DBCPANa3; CDBC=1 kg · m-3, CAgNO3 = 1.4 · 10−2 kg · m-3, [NaBH4]/[Ag+] = 80.

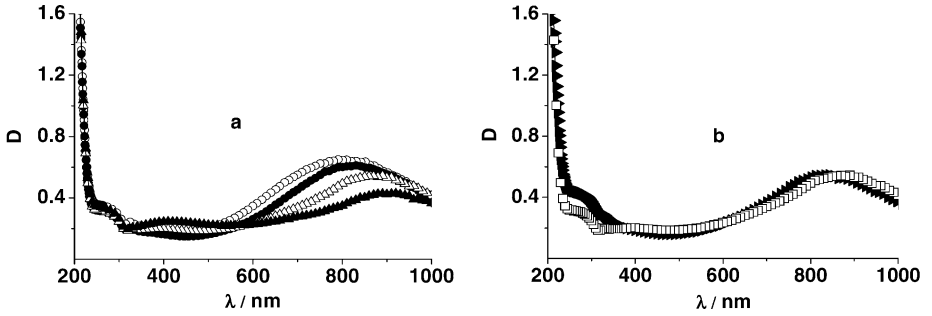

Figure 9.
Absorption spectra of (**a**) $Ag^+/DBC_{PAAc}3$ solutions in different times after $NaBH_4$ addition and also (**b**) $Ag^+/DBC_{PAAc}1$ and $Ag^+/DBC_{PAAc}3$ solutions through a certain time (120 min); (**a**) ○ = 5, • = 141, Δ = 1440, ▲ = 5760 min; (**b**) ▶ = $DBC_{PAAc}1$ □ = $DBC_{PAAc}3$. $C_{PAAc} = 1\,kg \cdot m^{-3}$, $C_{AgNO_3} = 1.4 \cdot 10^{-2}\,kg \cdot m^{-3}$, $[NaBH_4]/[Ag^+] = 80$.

realized in two distinct stages. At the first stage the reduction of Ag^+-ions and formation of primary nanoclusters and nanoparticles with a constant rate of $\sim 0.1 \div 0.04\,s^{-1}$ take place but at the second one the coagulation of primary clusters and nanoparticles occurs. The absence of any sediment in the reaction mixtures denoted the presence of fully stable silver dispersions. It should be noted that the reduction reaction in $DBC_{PANa}3$ solutions developed more actively than in the solutions of $DBC_{PANa}1$ that led to formation of a larger amount of silver nanoparticles (Figure 8e). Thus, the kinetics of the nanoparticle growth and their stability depended on PANa block length.

At the addition of the reducing agent to the mixtures of silver nitrate with DBC_{PAAc} samples in H-form (at the same ratio $[NaBH_4]/[Ag^+] = 80$) the solution pH became equaled to 6 that was accompanied by the destruction of initial DBC_{PAAc} micelles. UV-Vis spectra for corresponding reaction mixtures are shown in Figure 9.

The absorption bands near 400 nm were practically absent in these spectra. Instead them, the absorption bands in the region of $\lambda > 800\,nm$ (with $\lambda_{max} = 821\,nm$ for $DBC_{PAAc}1$ and $\lambda_{max} = 864\,nm$ for $DBC_{PAAc}3$) appeared. In fact, the formation of so-called ''blue silver'' took place in these cases. According to the literature data,[20] this result could be interpreted by the formation of very long sequences of the bound silver nanoclusters (and Ag^+ ions) along polyacid blocks of DBCs. From such point of view the ''blue silver'' is a product of the incomplete reduction of silver ions by sodium borohydride. Therefore, the chemical reduction of Ag^+ ions in DBC_{PAAc} solutions at pH ~ 6 (unlike to pH ~ 9) led to formation of silver nanoclusters and their complexes with polyacid blocks.

The main task of the last experimental series was to carry out the silver ion reduction in micellar structures of the copolymers. In order to solve this problem, we have decreased the molar ratio of $[NaBH_4]/[Ag^+]$ in the reaction mixture in 10 times (up to 8). In this case the solution pH = 3 was not changed. Results of these tests are represented in Figure 10.

At once after $NaBH_4$ addition, relatively broad absorption band with $\lambda_{max} = 431$–433 nm arose in the $Ag^+/DBC_{PAAc}3$ micellar solutions due to formation of silver nanoparticles. The intensity of this band was practically unchanged during some times (~24 h) and then disappeared because of the microphase separation in the system.

Evidently, that in DBC_{PAAc} micellar solutions at pH ~ 3 a very quick development of the reduction process and formation of Ag-nanoparticles with larger size (than in DBC_{PANa} solutions at pH ~ 9) took place.

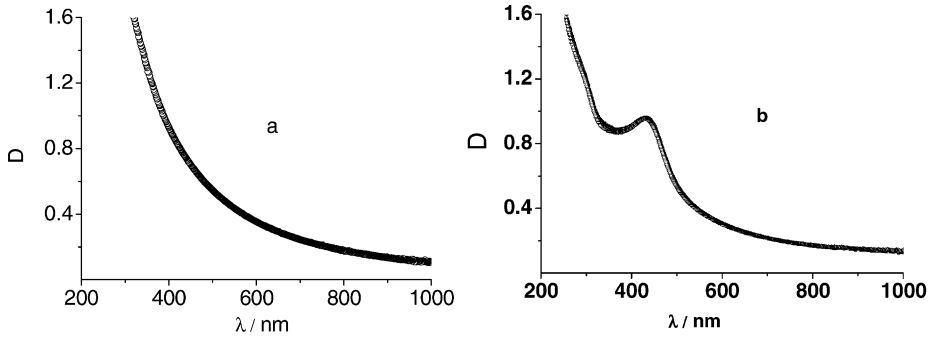

Figure 10.
Absorption spectra of (**a**) $Ag^+/DBC_{PAAc}3$ micellar solution without $NaBH_4$ and (**b**) in $5 \div 60$ min after $NaBH_4$ addition; $C_{PAAc} = 1\,kg \cdot m^{-3}$, $C_{AgNO3} = 1.4 \cdot 10^{-2}\,kg \cdot m^{-3}$, $[NaBH_4]/[Ag^+] = 8$.

Conclusion

Processes of block copolymerization of PAAc with MOPEG have a template character because the formation of the H-bond system between the propagating (''daughter's'') PAAc chains and MOPEO blocks. Template effects of DBCs syntheses were depended on the monomer concentrations in reaction mixture. The positive dynamic effects in the DBCs syntheses at relatively low monomer concentration ($<1.46\,mol \cdot dm^{-3}$) were appeared.

The given DBCs with interacting PAAc and MOPEO blocks were stimuli responsive copolymers. It was shown that the bulk structure of DBCs and their behavior in aqueous solutions strongly depended on the ionization degree of PAAc blocks. At low pH ($pH \leq 4$) PAAc blocks were protonated and connected with chemically complementary MOPEO blocks. Due to this, DBC macromolecules self-assembled into the micelles of different construction (with different nature of stabilizing ''corona'') in dependence on relative length of nonionic and polyacid blocks. The growth of micelle stability (the decrease in CMC and increase in $-\Delta G^\circ$ values) at the lowering asymmetric character of DBCs was established. The bulk structure of DBCs in H-form was fully homogeneous and amorphous because of interaction of both the blocks. At $pH \geq 6$ PAAc blocks were practically fully ionized; therefore, DBC macromolecules were in the isolated state in aqueous solutions. The bulk structure of DBC_{PANa} demonstrated a thermodynamic immiscibility of both the blocks.

The silver ion chemical reduction was carried out in DBC solutions at different pH and excess of sodium borohydride concentration in the reaction mixtures. Highly stable Ag nanoparticle dispersions were obtained with an excess of sodium borohydride ($[NaBH_4]/[Ag^+] =$ 8–80) in aqueous solutions of fully deprotonated DBC_{PANa} ($pH = 9.5$). Ag nanoparticle formation in DBC_{PAAc} micelles ($pH = 3$) under $[NaBH_4]/[Ag^+] = 8$ was established. It was revealed the partial reduction of Ag^+ to the nanoclusters and their further stabilization by partially protonated $DBC_{PAAc/PANa}$ ($pH = 6$). Thus, the functional capability of DBC_{PANa}, DBC_{PAAc} and $DBC_{PAAc/PANa}$ matrices to act as the templates for the silver nanoclusters/nanoparticles formation was shown.

[1] G. Riess, *Prog. Polym. Sci.* **2003**, *28*, 1107.
[2] H. Colfen, *Macromol. Rapid Commun.* **2001**, *22*(4), 219.
[3] S. Holappa, L. Kantonen, F. Winnik, H. Tenhu, *Macromolecules*, **2004**, *37*, 7008.

[4] M. Vamvakaki, L. Papoutsakis, V. Katsamanis, T. Afchoudia, P. Fragouli, H. Iatrou, N. Hadjichristidis, S. Armes, S. Sidorov, D. Zhirov, V. Zhirov, M. Kostylev, L. Bronstein, S. Anastasiadis, *Faraday Discuss.*, **2005**, *128*, 129.
[5] F. A. Plamper, J. R. McKee, A. Laukkanen, A. Nykänen, A. Walther, J. Ruokolainen, V. Aseyev, H. Tenhu, *Soft Matter*, **2009**, *5*, 1812.
[6] J.-F. Gofy, S. Varshney, R. Jerom, *Macromolecules*, **2001**, *34*, 3361.
[7] T. Zheltonozhskaya, N. Permyakova, et al. *Hydrogen-bonded interpolymer complexes. Formation, Structure, Applications*, V. V. Khutoryanskiy, G. Staikos, Eds., World Scientific Publishing Company, Singapore - London - New-Jersey etc, **2008**, Ch.5, 85.
[8] N. Permyakova, T. Zheltonozhskaya, N. Oboznova, *Molecular Cryst. Liquid Cryst.*, **2008**, *497*, 307.
[9] T. Zheltonozhskaya, N. Zagdanskaya, O. Demchenko, L. Momot, N. Permyakova, V. Syromyatnikov, L. Kunitskaya, *Russian Chemical Reviews*, **2004**, *73*(8), 813.
[10] I. Papisov, *Vysokomol. Soedin. Ser. B.* **1997**, *39*, 562.
[11] G. D. Poe, W. L. Jarrett, C. W. Scales, C. L. McCormick, *Macromolecules*, **2004**, *37*, 2603.
[12] V. Khutoryansky, A. Dubolazov, Z. Nucreeva, G. Mun, *Langmuir*, **2004**, *20*, 3785.
[13] J. Maurer, D. Eustace, C. Ratcliffe, *Macromolecules*, **1987**, *20*, 196.
[14] F. Meng, S. Zheng, T. Liu, *Polymer*, **2006**, *47*, 7590.
[15] E. Rufino, E. Monteiro, *Polymer*, **2000**, *41*, 4213.
[16] G. S. Haldankar, H. G. Spencer, *J. Appl. Polym. Science*, **1989**, *37*, 3137.
[17] H. Shen, L. Zang, A. Eisenberg, *J. Phys. Chem. B*, **1997**, *101*, 4697.
[18] K. Nakamoto, IR spectra and RS spectra of inorganic and coordination compounds, **1991**, Moscow, Mir, 536.
[19] E. Pretsch, Bullman, C. Affolter, Structure determination of organic compounds. Tablesofspectradata. Moscow, Mir **2006**.
[20] A. D. Pomogailo, A. S. Rozenberg, U. E. Uflynd, *Nanoscale metal particles in polymers*, **2000**, Moscow, Khimia, 672.
[21] B. V. Sergeev, L. I. Lopatina, et al. *Colloid. J.* **2005**, *67*(1), 79.
[22] D. G. Angelescu, M. Vasilescu, et al., *Colloids and surfaces: Physicochem. Eng. Aspects*, **2010**, 366.
[23] M. Moffitt, H. Vali, A. Eisenberg, *Chem. Mater.*, **1998**, *10*, 1021.
[24] Mie Plot ver. 4.01, http://www.philiplaven.com/mieplot.html.

